A Study of a Ruzicka Vibration Isolator Model with High-Static-Low-Dynamic Characteristic

Bingbing KANG*, Haijun LI**, Zhen ZHANG***, Hongyang ZHOU****
*Coast Defence Army Institute, Naval Aeronautical University, Yantai 264001, China, E-mail: 644925557@qq.com
**Coast Defence Army Institute, Naval Aeronautical University, Yantai 264001, China, E-mail: qingfeng_16@163.com
***Coast Defence Army Institute, Naval Aeronautical University, Yantai 264001, China, E-mail: 787026095@qq.com
****Department of Aviation Ammunition, Air Force Logistics College, Xuzhou 221000, China, E-mail:
891741851@qq.com

1. Introduction

With the development of precision instrument and equipment, the damage of low frequency vibration is more prominent. However, the traditional vibration isolator's ability in suppressing low frequency vibration is limited because of its large stiffness and high starting vibration isolation frequency. Although the reduction of the vibration isolator's stiffness could effectively solve the problem above, a trade-off between the load capacity and the vibration isolation performance is unavoidable. In order to solve the contradiction, growing attention is focused on high-static-low-dynamic vibration isolator. Its basic idea is introducing negative stiffness into the traditional vibration isolator. On the premise of guaranteeing vibration isolator's load capacity, its stiffness could be reduced close to zero under small vibration amplitude, which could isolate the low frequency vibration effectively. Related literature is as follows.

A. Carrella et al. [1] analyzed the simple quasi-zero-stiffness system composed by linear springs, and showed that the force could be approximated by a cubic equation of displacement; A. Carrella et al. [2] also analyzed the force transmissibility, with appropriate system parameters, the quasi-zero-stiffness isolator system could outperform the linear one; Ivana Kovacic et al. [3] studied the optimal combination of the quasi-zero stiffness parameters and analyzed the dynamic characteristics. Xingtian Liu et al. [4] used the pre-stressed Euler buckled beams to produce negative stiffness, which offset the positive stiffness of the linear spring to achieve the characteristic of quasi-zero stiffness; Jiaxi Zhou et al. [5] designed a quasi-zero stiffness vibration isolator with cam–roller–spring mechanisms, the piecewise nonlinear dynamic model's peak transmissibility and starting frequency won't overshoot those of corresponding linear systems; Ivana Kovacic et al. [6] investigated the effect of static force on quasi-zero stiffness. With the change of static force, some characteristics of hard stiffness and soft stiffness were developed. Chao-chieh Lan et al. [7] studied the influence of different loads on quasi-zero stiffness isolator and its adjustment mechanism to handle different loads; Xiuting Sun et al. [8] put forward a time-delayed active control strategy of the quasi-zero stiffness system, and this strategy could improve isolator's stability and transmissibility. Yingli et al. [9] studied floating raft isolation system with high-static-low-dynamic characteristic, and the vibration isolation performance was better than linear ones. Will S. Rob-

ertson et al. [10] added a magnetic spring into a vibration isolation system to realize high-static-low-dynamic characteristic, which has the properties of weak nonlinear and low inherent damping. Daolin Xu et al. [11] presented a magnetic isolator with high-static-low-dynamic characteristic and its performance in low-frequency domain is better than other vibration systems. Zhifeng Hao et al. [12] proposed a stable-quasi-zero-stiffness vibration isolator, in which SD oscillator was adopted to replace the Duffing system, and the precision of the large displacement vibration was improved. Jiaxi Zhou et al. [13] formed a pyramidal pillar with three compact quasi-zero stiffness springs and a 6-DOF QZS vibration isolator is established by 4 pyramidal pillars. Tao Zhu et al. [14] designed six degree of freedom (six-dof) vibration isolator with magnetic levitation as the payload support mechanism and achieved high-static-low-dynamic characteristic in all directions. Daolin Xu et al. [15] designed a flexible plate type isolator, which can eliminate resonance under certain damping. However, once these vibration isolator parameters are determined, it cannot be changed and high-static-low-dynamic mechanical properties will change under overload or underload condition, so Daolin Xu et al. [16] also put forward a kind of adjustable pneumatic vibration isolator. The air mass in cylinder can change according to specific load, making isolator keeping high-static-low-dynamic characteristic. But this paper did not study vibration isolator parameters' effect on the performance of vibration isolation.

With pneumatic high-static-low-dynamic vibration isolator as the research object, this paper studies the influence of parameter changes on the nonlinear mechanical properties. Based on this, we design a Ruzicka high-static-low-dynamic vibration isolation model and investigate its vibration isolation characteristics. In the calculation process of solving its amplitude-frequency characteristic, a new method – Harmonic Equivalent Linearization Method – is used, in which the equivalent linearization algorithm is introduced into Harmonic Balance Method. This method could greatly simplify the calculation process and gives the same result as Harmonic Balance Method. The effects of additional stiffness, damping and excitation amplitude on nonlinear amplitude-frequency characteristic are investigated numerically in Section 6.

2. Pneumatic vibration isolator model

A cylinder is used as an air spring, as shown in

Fig. 1. Fig. 1, a is double chamber spring; Fig. 1, b is single chamber spring. The spring consists of air chamber, air valve, piston, air vent, etc. The valve can change the mass of the air in the chamber and it is closed under the stable motion state. When the pneumatic spring is subjected to external forces, the piston rod moves, the volume and pressure of the air in the chamber changes.
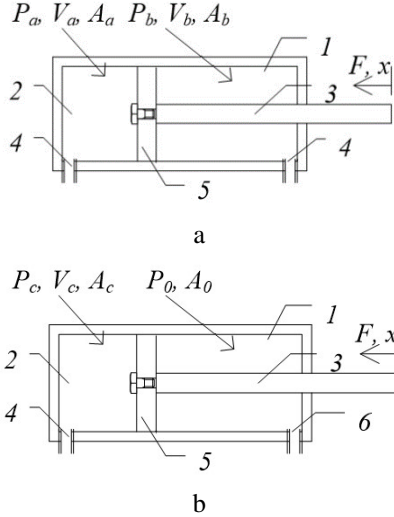

Fig. 1 Chamber spring: *1* - The upper air chamber, *2* - the lower air chamber, *3* - piston rod, *4* - air valve, *5* - piston, *6* - air vent

There is a state equation for the gas changing process without any condition:

$$P_1 V_1^r = P_2 V_2^r = const, \tag{1}$$

where: P_1, P_2 is the pressure and its unit is Pa; V_1, V_2 is the volume of gas and its unit is m³; r is the air polytrophic exponent. The polytrophic process of air in a pneumatic spring can be regarded as adiabatic, which means $r = 1.4$.

For a double-chamber air spring, we suppose the initial pressure of upper chamber is P_a, its volume is V_a, the piston's effective stressed area is A_a, and the corresponding notations of the lower chamber are P_b, V_b and A_b. The spring is in the stationary state at this time. If the pneumatic spring produces displacement x under the downward force F, the volume of the lower chamber is changed to:

$$V_{bm} = V_b - A_b x. \tag{2}$$

With Eqs. (1-2), the pressure in the gas chamber can be changed to:

$$P_{bm} = P_b \left(\frac{V_b}{V_b - A_b x} \right)^r. \tag{3}$$

In the same way, the volume and pressure of the upper chamber are changed to:

$$V_{am} = V_a + A_a x; \tag{4}$$

$$P_{am} = P_a \left(\frac{V_a}{V_a + A_a x} \right)^r. \tag{5}$$

So we can get the equation:

$$F = P_{bm} A_b - P_{am} A_a. \tag{6}$$

For a single-chamber air spring, we suppose the pressure of the upper chamber is P_0, which is a constant and the same as the atmospheric pressure, the piston's effective stressed area is A_0. The corresponding notations of the lower chamber are P_c and A_c, and its volume is V_c. We can get the same conclusion from the single-chamber air spring as that from the double-chamber air spring.

Because the upper chamber of the single air chamber spring is connected with the atmosphere, the force provided by the upper air chamber is a constant value. The upper air chamber of the double air chamber spring is closed, and the force it provides can be changed, which means that the double air chamber spring can provide more force under the same pressure condition, so the double air chamber spring is used in the vertical direction to support the load.

To achieve the high-static-low-dynamic property, this paper adopts the method of combined positive and negative stiffness, as shown in Fig. 2. The vibration isolator is composed of four horizontal single-chamber air springs and a vertical double-chamber air spring. l is the length of the horizontal swing arm. m is the mass of the loaded object. When the vibration isolator is in a static equilibrium position, the single-chamber springs would maintain at a horizontal position without providing any vertical force and the double-chamber spring supports the loaded object alone. When the base excitation creates displacement x_r, the vibration isolator would be disturbed and the loaded object would deviate from the equilibrium position with creating a displacement x_s.
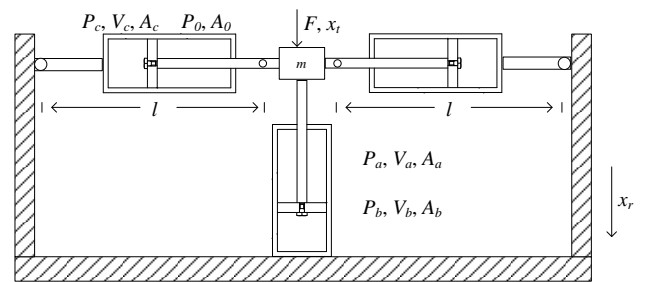

Fig. 2 Pneumatic high-static-low-dynamic vibration isolator

If the vibration isolator is not disturbed by external forces, it would be at equilibrium position and the equation is:

$$mg = P_b A_b - P_a A_a. \tag{7}$$

3. Static analysis of pneumatic vibration isolator

When the loaded object in the equilibrium position is affected by external force F, the displacement x is generated, and the following relation is expressed as:

$$F = -4 \left[P_c \left(\frac{V_c}{V_c + A_c \sqrt{x^2 + l^2} - A_c l} \right)^r A_c - P_0 A_0 \right] \frac{x}{\sqrt{x^2 + l^2}} + mg - P_b \left(\frac{V_b}{V_b + xA_b} \right)^r A_b + P_a \left(\frac{V_a}{V_a - xA_a} \right)^r A_a. \tag{8}$$

Suppose the initial height of the double-chamber spring's upper chamber is $h_a = V_a / A_a$, that of the lower one is $h_b = V_b / A_b$, and the initial height of the single-chamber spring's lower chamber is $h_c = V_c / A_c$. Set $\hat{F} = F / P_0 A_0$, $\lambda_c = P_c A_c / P_0 A_0$, $\lambda_b = P_b A_b / P_0 A_0$, $\lambda_a = P_a A_a / P_0 A_0$, $\lambda_m = mg / P_0 A_0$, $\hat{h}_c = h_c / l$, $\hat{x} = x / l$, $\hat{h}_a = h_a / l$, $\hat{h}_b = h_b / l$, then Eq. (8) simplifies to:

$$\hat{F} = -4H_1 \frac{\hat{x}}{\sqrt{\hat{x}^2 + 1}} + \lambda_m - \lambda_b H_2 + \lambda_a H_3, \tag{9}$$

where:

$$H_1 = \lambda_c \left[\hat{h}_c / \left(\hat{h}_c + \sqrt{\hat{x}^2 + 1} - 1 \right) \right]^r - 1, \quad H_2 = \left[\hat{h}_b / \left(\hat{h}_b + \hat{x} \right) \right]^r,$$

$$H_2 = \left[\hat{h}_a / \left(\hat{h}_a - \hat{x} \right) \right]^r.$$

Taking the derivative of Eq. (9) subject to $\hat{x}$, we can get the equation of stiffness $\hat{k}$ and $\hat{x}$:

$$\hat{k} = 4H_1 \left[\hat{x}^2 \left(\frac{1}{\sqrt{\hat{x}^2 + 1}} \right)^3 - \frac{1}{\sqrt{\hat{x}^2 + 1}} \right] + \frac{\lambda_b r}{\hat{h}_b + \hat{x}} H_2 +$$

$$+ \frac{\lambda_a r}{\hat{h}_a - \hat{x}} H_3 + \frac{\hat{x}^2}{\hat{x}^2 + 1} \frac{4\lambda_c h_c^r r}{\left(\hat{h}_c + \sqrt{\hat{x}^2 + 1} - 1 \right)^{r+1}}. \tag{10}$$

In order to ensure that the vibration isolator has the high-static-low-dynamic characteristic, the vibration isolator must be 0 stiffness in the equilibrium position and no negative stiffness all the time. In other words, when $x=0$, $F=0$, $k=0$ and $k=0$ is the local minimum, the equation set is:

$$\left. \begin{array}{l} \hat{k}' = -\dfrac{\lambda_b r(r+1)}{\hat{h}_b^2} + \dfrac{\lambda_a r(r+1)}{\hat{h}_a^2} = 0 \\[2mm] \hat{F} = \lambda_m - \lambda_b + \lambda_a = 0 \\[2mm] \hat{k} = \dfrac{\lambda_b r}{\hat{h}_b} + \dfrac{\lambda_a r}{\hat{h}_a} - 4\lambda_c + 4 = 0 \end{array} \right\}. \tag{11}$$

So, Eq. set (11) becomes:

$$\lambda_m = \lambda_b - \frac{\hat{h}_a^2 \lambda_b}{\hat{h}_b^2}, \lambda_b = \frac{\hat{h}_b^2 \lambda_m}{\hat{h}_b^2 - \hat{h}_a^2}$$

$$\lambda_c = 1 + \frac{1}{4} \left(\frac{\lambda_b (\hat{h}_a + \hat{h}_b) r}{\hat{h}_b^2} \right) = 1 + \frac{\lambda_m r}{4 \left(\hat{h}_b - \hat{h}_a \right)}. \tag{12}$$

$$\lambda_a / \lambda_b = \hat{h}_a^2 / \hat{h}_b^2$$

Because $\lambda_b > 0$, so $\hat{h}_b > \hat{h}_a$.
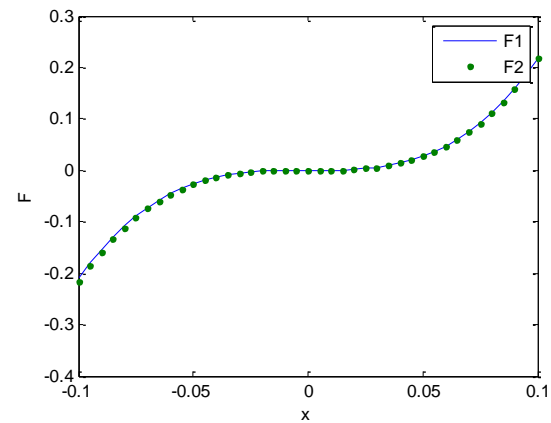Substituting Eq. (12) into Eq. (19) gives:

$$\hat{F} = -4 \left[\left(1 + \frac{\lambda_m r}{4\hat{h}_b - 4\hat{h}_a} \right) \left(\frac{\hat{h}_c}{\hat{h}_c + \sqrt{\hat{x}^2 + 1} - 1} \right)^r - 1 \right] \frac{\hat{x}}{\sqrt{\hat{x}^2 + 1}} + \lambda_m - \frac{\hat{h}_b^2 \lambda_m}{\hat{h}_b^2 - \hat{h}_a^2} \left(\frac{\hat{h}_b}{\hat{h}_b + \hat{x}} \right)^r + \frac{\hat{h}_a^2 \lambda_m}{\hat{h}_b^2 - \hat{h}_a^2} \left(\frac{\hat{h}_a}{\hat{h}_a - \hat{x}} \right)^r. \tag{13}$$

Expand Eq. (13) in third order Taylor:

$$\hat{F} = \frac{1}{6} \left[\frac{\lambda_m r(r+1)(r+2)}{\hat{h}_a \left(\hat{h}_b^2 - \hat{h}_a^2 \right)} + \frac{\lambda_m r(r+1)(r+2)}{\hat{h}_b \left(\hat{h}_b^2 - \hat{h}_a^2 \right)} + \frac{3\lambda_m r}{\hat{h}_b - \hat{h}_a} + \frac{r}{\hat{h}_c} \left(12 + \frac{3\lambda_m r}{\hat{h}_b - \hat{h}_a} \right) \right] \hat{x}^3. \tag{14}$$

Assume the parameters' values of the vibration isolator are: m=100 kg; P_0=0.101 MPa; A_0=0.286×10^{-3} m^3; A_a=1.7624×10^{-3} m^3; A_b=1.9635×10^{-3} m^3; A_c=0.314×10^{-3} m^3; h_a=0.06 m; h_b=0.14 m; h_c=0.02 m; l=0.08 m and the corresponding dimensionless parameters' values are $\hat{h}_b = 1.75$, $\hat{h}_c = 0.25$, $\hat{h}_a = 0.75$, $\lambda_m = 33.93$.

In order to verify the error of Eq. (14) is small enough, we compare Eq. (14) to (13) with the numerical method using the above values. Fig. 3 shows the relationship diagram of the dimensionless force and displacement, where $F1$ represents the Eq. (13) and $F2$ represents the Eq. (14). Fig. 4 shows the relationship diagram of dimensionless stiffness and displacement, where $K1$ represents the Eq. (13) and $K2$ represents the Eq. (14). As we can see from the figures, the third order Taylor expansion is a good representation of Eq. (13) under the small amplitude condition ($\hat{x} \leq 0.1$), which means error of Eq. (14) is small enough.

Fig. 3 The relationship between dimensionless force and displacement

Suppose $T = \dfrac{\lambda_m r(r+1)(r+2)}{\hat{h}_a\left(\hat{h}_b^2 - \hat{h}_a^2\right)} + \dfrac{\lambda_m r(r+1)(r+2)}{\hat{h}_b\left(\hat{h}_b^2 - \hat{h}_a^2\right)} + \dfrac{3\lambda_m r}{\hat{h}_b - \hat{h}_a} + \dfrac{r}{\hat{h}_c}\left(12 + \dfrac{3\lambda_m r}{\hat{h}_b - \hat{h}_a}\right)$, take partial derivative T with respect to $\hat{h}_a$, $\hat{h}_b$, $\hat{h}_c$ respectively:

$$\frac{dT}{d\hat{h}_a} = \frac{3\lambda_m r}{\left(\hat{h}_b - \hat{h}_a\right)^2} + \frac{3\lambda_m r^2}{\hat{h}_c\left(\hat{h}_b - \hat{h}_a\right)^2} + \frac{2\lambda_m r(r+1)(r+2)}{\left(\hat{h}_b^2 - \hat{h}_a^2\right)^2} + \frac{\lambda_m r(r+1)(r+2)}{\hat{h}_a^2\left(\hat{h}_b^2 - \hat{h}_a^2\right)} + \frac{2\hat{h}_a\lambda_m r(r+1)(r+2)}{\hat{h}_b\left(\hat{h}_b^2 - \hat{h}_a^2\right)^2} > 0, \quad (15)$$

$$\frac{dT}{d\hat{h}_b} = -\frac{\lambda_m r(r+1)(r+2)}{\hat{h}_b^2\left(\hat{h}_b^2 - \hat{h}_a^2\right)} - \frac{3\lambda_m r^2}{\hat{h}_c\left(\hat{h}_b - \hat{h}_a\right)^2} - \frac{3\lambda_m r}{\left(\hat{h}_b - \hat{h}_a\right)^2} - \frac{2\lambda_m r(r+1)(r+2)}{\left(\hat{h}_b - \hat{h}_a\right)^2} - \frac{2\hat{h}_b\lambda_m r(r+1)(r+2)}{\hat{h}_a\left(\hat{h}_b^2 - \hat{h}_a^2\right)^2} < 0, \quad (16)$$

$$\frac{dT}{d\hat{h}_c} = \left(-\frac{3\lambda_m r^2}{\hat{h}_b - \hat{h}_a} - 12r\right)\frac{1}{\hat{h}_c^2} < 0. \quad (17)$$
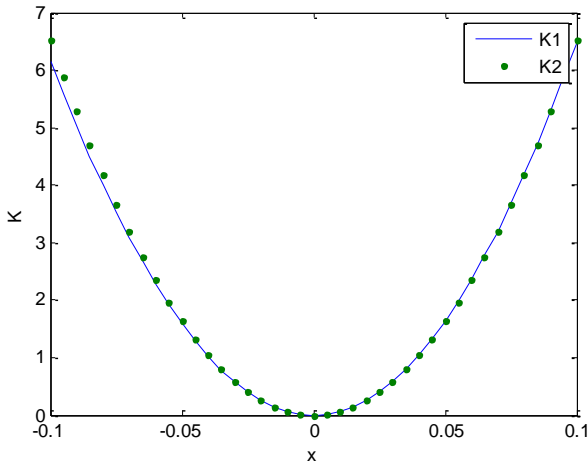

Fig. 4 The relationship between dimensionless stiffness and displacement

Because there is no l in the dimensionless force, in this case, we cannot judge the influence of l on vibration isolator. So Eq. (14) needs to be dimensioned, and the partial derivative of the third order's coefficient subject to l is:

$$\frac{d\bar{T}}{dl} = \frac{P_0 A_0}{6}\left[\frac{-6mgr}{l^3\left(h_b - h_a\right)} - \frac{24r}{l^3 h_c} - \frac{3mgr^2}{l^2 h_c\left(h_b - h_a\right)}\right] < 0. \quad (18)$$

Therefore, it can be concluded that, when the engineering conditions permit, decreasing T, that is, increasing $\hat{h}_b$, $\hat{h}_c$ or decreasing $\hat{h}_a$, λ_m (increasing h_b, h_c, A_0 or decreasing h_a, l), can expand the amplitude region of the vibration isolator with high-static-low-dynamic characteristic.

4. Ruzicka high-static-low-dynamic vibration isolator model

The traditional high-static-low-dynamic vibration isolator model can be simplified as shown in Fig. 5, which is quasi-zero and nonlinear. x is the displacement of the isolated object with mass m, y is the base excitation displacement, c is the system damping, k_0 is the nonlinear stiffness, and z is the displacement of the damper. Fig. 5 is simplified figure of Fig. 2.

The Ruzicka high-static-low-dynamic vibration isolator model established in this paper, as shown in Fig. 6, can be generated by adding a spring into the traditional one. k_2 is the stiffness of the added spring. When k_2 is 0, the vibration isolator in Fig. 6 is equivalent to a model without a damper; when k_2 is infinite, the model in Fig. 6 is the same as that in Fig. 5.

5. A new method to solve the model's vibration amplitude-frequency characteristic

To solve the vibration amplitude-frequency characteristic of the model above, there are many methods such as Harmonic Balance Method, Perturbation Method, Averaging Method, Multiple Scale Method. However, their calculation process is very complex. In this section, a new method is introduced to simplify the calculation process, which gives the same results as Harmonic Balance Method. In this Section, we assume that the vibration amplitude is as small as we discussed in Section 3, so nonlinear spring restoring force can be expressed as a third order Taylor formula.
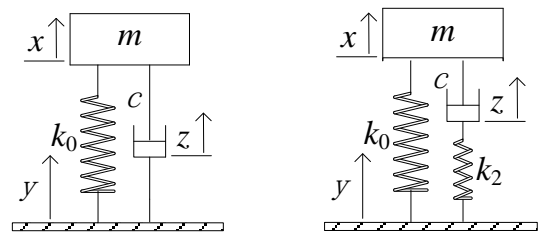

Fig. 5 vibration isolator   Fig. 6 Ruzicka vibration isolator

5.1. The new method – Harmonic Equivalent Linearization Method

The new method is called Harmonic Equivalent Linearization Method. In this method, the equivalent linearization algorithm [17] is introduced into Harmonic balance method. As a result, the nonlinear equation is equivalent to the linear equation with the same results, and the calculation process is greatly simplified. This method is applied to solve the main resonance response of the Duffing equation.

The calculation process of the new method is as following.

Suppose the dynamics Duffing equation of the Ruzicka high-static-low-dynamic vibration isolator is:

$$mx'' + c(x' - z') + k_1(x - y) + k_3(x - y)^3 = 0, \qquad (19)$$

$$c(x' - z') = k_2(z - y), \qquad (20)$$

where: $k_1(x - y) + k_3(x - y)^3$ is nonlinear spring restoring force in the form of Eq. (14), we get Eqs. (19-20) by force analysis of the isolator in Fig. 6. If the natural frequency shown in Fig. 6 is w_0, then the nonlinear spring restoring force $k_1(x - y) + k_3(x - y)^3$ could be equivalent to $k_0(x - y)$, so $k_0 = mw_0^2$ and Eqs. (19-20) could be equivalent to:

$$x'' + 2\xi w_0(x' - z') + w_0^2(x - y) = 0, \qquad (21)$$

$$2\xi w_0(x' - z') = \bar{k}_2(z - y), \qquad (22)$$

where: $\xi = \dfrac{c}{2\sqrt{mk_0}}$, $2\xi w_0 = \dfrac{c}{m}$, $\bar{k}_2 = k_2/m$.

Therefore, the nonlinear equation could be solved as a linear equation by obtaining the natural frequency of Fig. 6.

Setting $\tau = w_0 t$, $\bar{k}_1 = k_1/m$, $\bar{k}_3 = k_3/m$, the free vibration equation of Fig. 6 is:

$$w_0^2 x''(\tau) + \bar{k}_1 x(\tau) + \bar{k}_3 x^3(\tau) = 0, \qquad (23)$$

where: $x(\tau)$ is a periodic function with a period of 2π.

The solution of Eq. (8) can be written in form as:

$$x(\tau) = x_1(\tau) + \Delta x(\tau), \qquad (24)$$

Then the transfer functions are written as:

$$G_1(s) = \frac{R(s)}{Y(s)} = -\frac{2\xi w_0 s^3}{2\xi w_0 s^3 + \bar{k}_2 s^2 + 2\xi w_0 \bar{k}_2 s + 2\xi w_0^3 s + w_0^2 \bar{k}_2}, \qquad (32)$$

$$G_2(s) = \frac{X(s)}{Y(s)} = \frac{2\xi w_0 \bar{k}_2 s + 2\xi w_0^3 s + w_0^2 \bar{k}_2}{2\xi w_0 s^3 + \bar{k}_2 s^2 + 2\xi w_0 \bar{k}_2 s + 2\xi w_0^3 s + w_0^2 \bar{k}_2}, \qquad (33)$$

$$G_3(s) = \frac{P(s)}{Y(s)} = -\frac{\bar{k}_2 s^2}{2\xi w_0 s^3 + \bar{k}_2 s^2 + 2\xi w_0 \bar{k}_2 s + 2\xi w_0^3 s + w_0^2 \bar{k}_2}. \qquad (34)$$

Amplitude ratios are given as:

$$\beta_1 = \frac{R}{Y} = \frac{2\xi w_0 w^3}{\sqrt{(2\xi w_0 w)^2 (w_0^2 + \bar{k}_2 - w^2)^2 + \bar{k}_2^2 (w_0^2 - w^2)^2}}, \qquad (35)$$

$$\beta_2 = \frac{X}{Y} = \frac{\sqrt{(2\xi w_0 w)^2 (\bar{k}_2 + w_0^2)^2 + \bar{k}_2^2 w_0^4}}{\sqrt{(2\xi w_0 w)^2 (w_0^2 + \bar{k}_2 - w^2)^2 + \bar{k}_2^2 (w_0^2 - w^2)^2}}, \qquad (36)$$

$$\beta_3 = \frac{P}{Y} = \frac{\bar{k}_2 w^2}{\sqrt{(2\xi w_0 w)^2 (w_0^2 + \bar{k}_2 - w^2)^2 + \bar{k}_2^2 (w_0^2 - w^2)^2}}, \qquad (37)$$

where: $x_1(\tau)$ is the first-order approximation solution, $\Delta x(\tau)$ is the minor error correction of the solution.

We define:

$$x_1(\tau) = A \cos \tau. \qquad (25)$$

Substituting Eq. (25) into Eq. (23) and ignoring the higher order terms of $\Delta x(\tau)$ give:

$$w_0^2 \Delta x''(\tau) + \bar{k}_1 \Delta x(\tau) + \bar{k}_3 (A \cos \tau)^2 \Delta x(\tau) - \\ -w_0^2 A \cos \tau + \bar{k}_1 A \cos \tau + \bar{k}_3 (A \cos \tau)^3 = 0. \qquad (26)$$

If $\Delta x(\tau) = 0$, Using Harmonic Balance Method with ignoring the higher order harmonics and setting the coefficient of the first order harmonic term to be 0, implies the first order approximation of the natural frequency is:

$$w_0^2 = \bar{k}_1 + \frac{3\bar{k}_3 A^2}{4}. \qquad (27)$$

Define $r = z-y$; $p = x-z$; $y = Y\cos wt$; $x = X\cos(wt + \Theta_1)$; $p = P\cos(wt + \Theta_2)$; $r = R\cos(wt + \Theta_3)$, Eqs. (19-20) become:

$$(p + r + y)'' + 2\xi w_0 p' + w_0^2(p + r) = 0, \qquad (28)$$

$$2\xi w_0 p' = \bar{k}_2 r. \qquad (29)$$

The Laplace transform of Eqs. (28-29) is:

$$[P(s) + R(s) + Y(s)]s^2 + 2\xi w_0 s P(s) + \\ + w_0^2 [P(s) + R(s)] = 0. \qquad (30)$$

$$2\xi w_0 s P(s) = \bar{k}_2 R(s). \qquad (31)$$

where $w_0^2 = \bar{k}_1 + \dfrac{3\bar{k}_3 A^2}{4}$, A is amplitude of $x - y$.

5.2. The merit of Harmonic Equivalent Linearization Method

Firstly, we will compare the calculation results of the new method with that of Harmonic Balance Method.

If the Harmonic Balance Method is used to calculate Eqs. (19-20), Eqs. (19-20) can be expressed as follows:

$$(p + r + y)'' + \bar{c}p' + \bar{k}_1(p + r) + \bar{k}_3(p + r)^3 = 0, \qquad (38)$$

$$\bar{c}p' = \bar{k}_2 r. \qquad (39)$$

Similarly, define $r = z - y$; $p = x - z$; $y = Y\cos wt$; $x = X\cos(wt + \Theta_1)$, so $x = p + r + y$. Let $p = P\cos(wt + \Theta_2)$; $r = R\cos(wt + \Theta_3)$ and and it can be obtained by Eq. (39) that

$$r = -\frac{\bar{c}wP}{k_2}\sin(wt + \theta_2) \text{ , so:}$$

$$p + r = P\sqrt{1 + \frac{\bar{c}^2 w^2}{\bar{k}_2^2}}\cos(wt + \theta + \theta_2), \qquad (40)$$

where: $\cos\theta = \left(1 + \dfrac{\bar{c}^2 w^2}{\bar{k}_2^2}\right)^{-\frac{1}{2}}$, $\sin\theta = \dfrac{\bar{c}w}{k_2}\left(1 + \dfrac{\bar{c}^2 w^2}{\bar{k}_2^2}\right)^{-\frac{1}{2}}$.

Substituting Eq. (40) into Eq. (38) gives:

$$-w^2\left[P\cos(wt + \theta) - \frac{\bar{c}wP}{\bar{k}_2}\sin(wt + \theta) + Y\cos wt\right] - \bar{c}wP\sin(wt + \theta) +$$

$$+\bar{k}_1\left[P\cos(wt + \theta) - \frac{\bar{c}wP}{\bar{k}_2}\sin(wt + \theta)\right] + \bar{k}_3\left[P\sqrt{1 + \frac{\bar{c}^2 w^2}{\bar{k}_2^2}}\cos(wt + \theta + \theta_1)\right]^3 = 0. \qquad (41)$$

Using Harmonic Balance Method with ignoring the higher order harmonics and setting the coefficient of the first order harmonic term to be 0 gives:

$$-w^2\left[P\cos\theta - \frac{\bar{c}wP}{\bar{k}_2}\sin\theta + Y\right] - \bar{c}wP\sin\theta + \bar{k}_1\left[P\cos\theta - \frac{\bar{c}wP}{\bar{k}_2}\sin\theta\right] +$$

$$+\frac{3\bar{k}_3}{4}\left[P\sqrt{1 + \frac{\bar{c}^2 w^2}{\bar{k}_2^2}}\right]^3\left[\cos(wt + \theta)\left(1 + \frac{\bar{c}^2 w^2}{\bar{k}_2^2}\right)^{-\frac{1}{2}} - \sin(wt + \theta)\frac{\bar{c}w}{k_2}\left(1 + \frac{\bar{c}^2 w^2}{\bar{k}_2^2}\right)^{-\frac{1}{2}}\right] = 0, \qquad (42)$$

$$-w^2\left[-P\sin\theta - \frac{\bar{c}wP}{\bar{k}_2}\cos\theta\right] - \bar{c}wP\cos\theta + \bar{k}_1\left[-P\sin\theta - \frac{\bar{c}wP}{\bar{k}_2}\cos\theta\right] +$$

$$+\frac{3\bar{k}_3}{4}\left[P\sqrt{1 + \frac{\bar{c}^2 w^2}{\bar{k}_2^2}}\right]^3\left[-\left(1 + \frac{\bar{c}^2 w^2}{\bar{k}_2^2}\right)^{-\frac{1}{2}}\sin\theta - \frac{\bar{c}w}{k_2}\left(1 + \frac{\bar{c}^2 w^2}{\bar{k}_2^2}\right)^{-\frac{1}{2}}\cos\theta\right] = 0, \qquad (43)$$

where: $w_0^2 = \bar{k}_1 + \dfrac{3}{4}\bar{k}_3 P^2\left(1 + \dfrac{\bar{c}^2 w^2}{\bar{k}_2^2}\right)$. Substituting it into Eq. (43) gives:

$$\tan\theta = \left[-\bar{c}w^3 + \bar{c}wk_2 + \bar{c}ww_0^2\right]\big/\left[w^2 - w_0^2\right]\bar{k}_2. \qquad (44)$$

Substituting Eq. (44) into Eq. (42) gives:

$$\frac{P}{Y} = \frac{\bar{k}_2 w^2}{\sqrt{\bar{k}_2^2\left(w^2 - w_0^2\right)^2 + \left(-\bar{c}w^3 + \bar{c}w\bar{k}_2 + \bar{c}ww_0^2\right)^2}}. \qquad (45)$$

Substituting Eq. (45) into Eq. (40) gives:

$$\frac{R}{Y} = \frac{2\xi w_0 w^3}{\sqrt{(2\xi w_0 w)^2(w_0^2 + \bar{k}_2 - w^2)^2 + \bar{k}_2^2(w_0^2 - w^2)^2}}. \qquad (46)$$

Substituting Eqs. (44-46) into equation $x = p + r + y$ gives:

$$\frac{X}{Y} = \frac{\sqrt{(2\xi w_0 w)^2(\bar{k}_2 + w_0^2)^2 + \bar{k}_2^2 w_0^4}}{\sqrt{(2\xi w_0 w)^2(w_0^2 + \bar{k}_2 - w^2)^2 + \bar{k}_2^2(w_0^2 - w^2)^2}}. \qquad (47)$$

It can be seen that Harmonic Balance Method have the same solutions as the new method, Harmonic Equivalent Linearization Method.

Secondly, if we pay attention to the calculation details, we can easily get the conclusion that the calculation process of the new method is much easier than that of Harmonic Balance Method.

In a world, the new method could greatly simplify the calculation process and gives the same results as Harmonic Balance Method in solving the main resonance response of Duffing equation.

6. Analysis of the model's vibration amplitude-frequency characteristic

Based on Eq. (36), which is obtained with Harmonic Equivalent Linearization Method, though there is no analytical solution, this section analyzes the influence of parameters' changes on the amplitude-frequency characteristic by numerical method. Because Eq. (36) is the stable solution of the vibration response, we do not consider the effect of the initial displacement and velocity of the vibration in this Section.

6.1. Effect of additional stiffness on amplitude-frequency characteristic

Using the data in section 3 implies $\bar{k}_3 = 1.22 \times 10^5$, $\bar{k}_1 = 0$. We assume that damping c is nonlinear, and the damping ratio is constant. Let $\xi = 0.1$, $Y = 0.001$ and $\bar{k}_2$ = 0, 0.01, 0.1, 1, 10, ∞. The effect of additional stiffness on logarithmic amplitude-frequency characteristic can be obtained from Eq. (36), which is shown in Fig. 7. It can be seen from the figure that, with the increase of additional stiffness, both the jump-down frequency and resonance peak are reduced, maximum with $\bar{k}_2 = 0$ and minimum with $\bar{k}_2 = \infty$. In the non-resonant part, amplitude transfer rate is reduced with the increase of $\bar{k}_2$, and the higher the frequency, the greater the difference. But in the vicinity of $w = 0$, the amplitude transfer rate of $\bar{k}_2 = 0.1$ is higher than that of $\bar{k}_2$ = 1, 10, ∞. In the whole frequency band, there is not much difference in amplitude transfer rate between $\bar{k}_2 = 10$ and $\bar{k}_2 = \infty$.
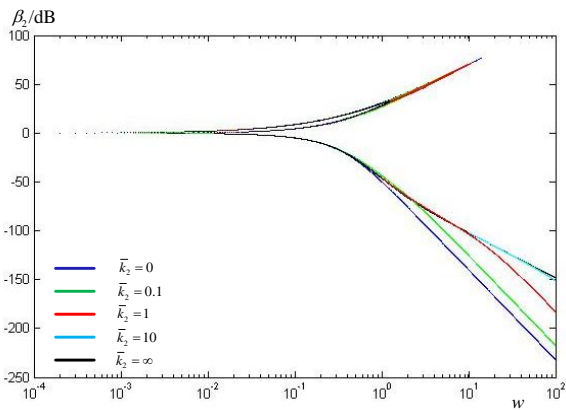

Fig. 7 The effect of additional stiffness on logarithmic amplitude-frequency characteristic under non-linear damping condition

For linear damping, let $c = 0.018$ and $\bar{k}_2$ = 0, 0.01, 0.1, 1, 10. The effect of additional stiffness on logarithmic amplitude-frequency characteristic obtained from Eq. (36) is shown in Fig. 8, which is similar to that in Fig. 7.
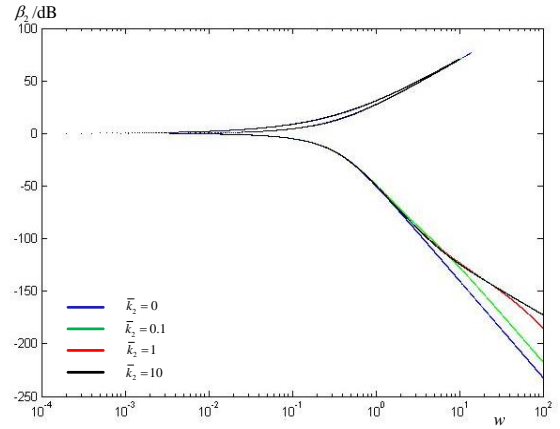

Fig. 8 The effect of additional stiffness on logarithmic amplitude-frequency characteristic under linear damping condition

6.2. Effect of damping on amplitude-frequency characteristic

Let $Y = 0.001$, $\bar{k}_2 = 0.1$ and ξ = 0, 0.01, 0.1, 0.5, 1. The effect of under-damping on logarithmic amplitude-frequency characteristic obtained from Eq. (36) is shown in Fig. 9. Under the condition of under-damping, with the increase of damping ratio, the resonance peak of amplitude-frequency characteristic curve decreases. When $\xi = 1$, there is a noncontinuous curve and the complete curve is shown in Fig. 10. In non-resonant part, amplitude transfer rate is decreasing with the decrease of the damping ratio. Except for the curve with $\xi = 0$, as the frequency increases, the amplitude-frequency characteristic curves converge to the curve of $\xi = 1$.
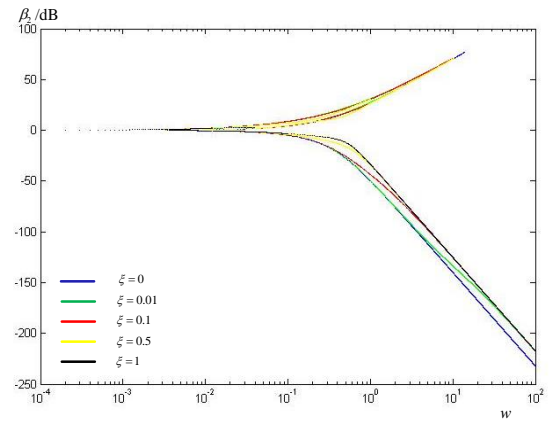

Fig. 9 The effect of under-damping on logarithmic amplitude-frequency characteristic

Under the condition of over-damping, let ξ = 1, 5, 10. The effect of over-damping on logarithmic amplitude-frequency characteristic obtained from Eq. (36) is shown in Fig. 10. It can be seen from the figure that, in the outer region of the dotted line, the damping ratio has no obvious effect on the amplitude-frequency characteristic. In the inner region of the dotted line, it is discontinuous between the upper branch and the lower branch of the amplitude-frequency characteristic curve. With the increase of damping ratio, the upper branch is closer to the lower

branch. Because of discontinuity, the amplitude-frequency characteristic can only jump from the upper branch to the lower one. Therefore, the resonance can be suppressed by controlling the initial state of vibration.
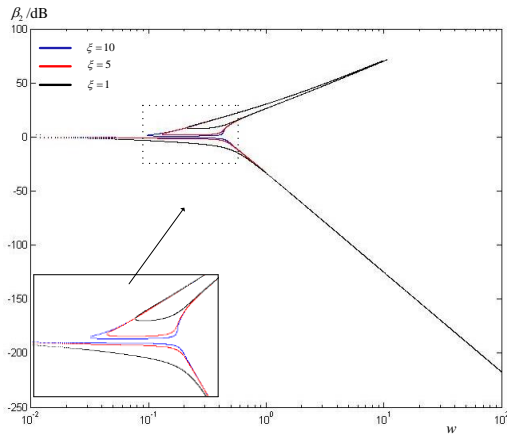

Fig. 10 The effect of over-damping on logarithmic amplitude-frequency characteristic

6.3. Effect of base excitation amplitude on amplitude-frequency characteristic

Let $\bar{k}_2 = 0.1$, $\xi = 1$ and $Y = 0.01$, 0.005, 0.001. The effect of base excitation amplitude on logarithmic amplitude-frequency characteristic obtained from Eq. (36) is shown in Fig. 11. We can get that the bigger the base excitation amplitude is, the worse the effect of vibration isolation is. And the Ruzicka high-static-low-dynamic vibration isolator put forward in this paper can only be applied to small amplitude situations.
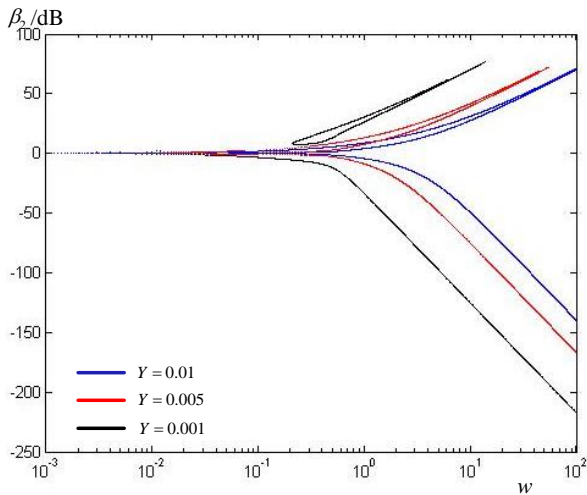

Fig. 11 The effect of base excitation amplitude on logarithmic amplitude-frequency characteristic

6.4. Analysis of simulation experiment

In order to verify the accuracy of Eq. (36), the vibration simulation based on Matlab\Simulink is constructed, as shown in the Fig. 12.
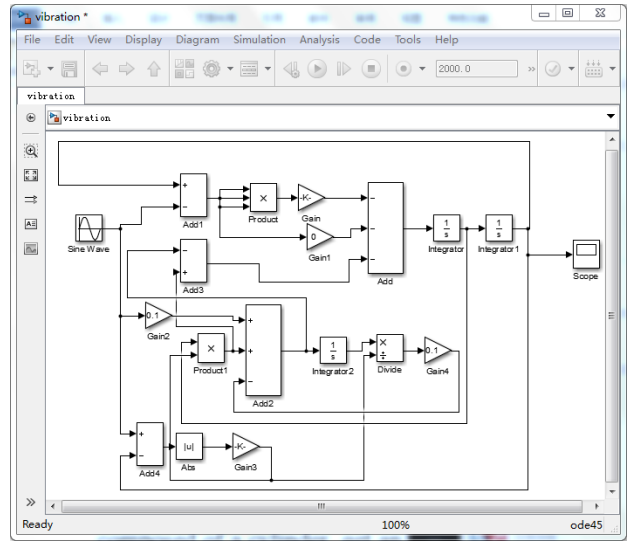

Fig. 12 The vibration simulation based on Simulink

Let $\bar{k}_2 = 0.1$, $\xi = 1$ and $Y = 0.001$. For the simulation, the initial velocity is 0, and the initial displacement is the vibration equation solution. The equation solution and simulation solution are shown in Fig. 13. In the non-resonant segment, the simulation solution is stable, as shown in figure 13; in the resonance segment, the simulation appears chaotic phenomenon, which is not marked in the figure. It can be seen from the figure, the stable solutions of simulation and equation are similar, which means the credibility of the equation solution is higher, and also verified that the resonance can be suppressed by controlling the initial state of vibration.
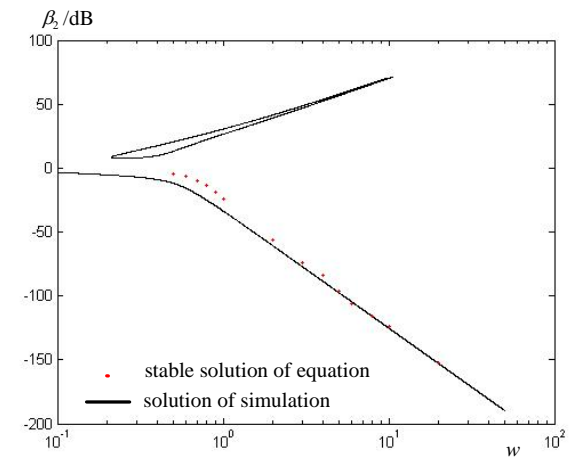

Fig. 13 Logarithmic amplitude-frequency characteristic based on simulation

7. Conclusion

This paper studies a Ruzicka vibration isolator model with high-static-low-dynamic characteristic. Firstly, we analyze mechanical property of the quasi-zero stiffness spring which is composed of a cylinder, get an approximate expression of the spring's static force. This kind of spring is the main part of a high-static-low-dynamic vibration isolator. Also we concluded that, when the engineering conditions permit, decreasing T, that is, increasing $\hat{h}_b$,

$\hat{h}_c$ or decreasing $\hat{h}_a$, λ_m (increasing h_b, h_c, A_0 or decreasing h_a, l), can expand the amplitude region of the vibration isolator with high-static-low-dynamic characteristic. Secondly, a Ruzicka high-static-low-dynamic vibration isolator with Duffing equation is put forward, which is a combination of a Ruzicka vibration isolator and a high-static-low-dynamic vibration isolator. In the calculation process of solving its amplitude-frequency characteristic, a new method — Harmonic Equivalent Linearization Method — is used, in which the equivalent linearization algorithm is introduced into Harmonic Balance Method. This method could greatly simplify the calculation process and gives the same results as Harmonic Balance Method in solving the main resonance response of Duffing equation. Finally, the effects of additional stiffness, damping and excitation amplitude on nonlinear amplitude-frequency characteristic are investigated numerically, and also verified that the stable solutions of simulation and equation are similar. The results show that the Ruzicka high-static-low-dynamic vibration isolator is suitable for small amplitude vibration. The appropriate additional stiffness and damping ratio can change the resonance band of the amplitude-frequency characteristic curve. The amplitude-frequency characteristic can only jump from the upper branch to the lower one. Therefore, the resonance can be suppressed by controlling the initial state of vibration.

References

1. **Carrella, A.; Brennan, M. J.; Waters, T P.** 2007. Static analysis of a passive vibration isolator with quasi-zero-stiffness characteristic, Journal of Sound and Vibration 301: 678-689.
   https://doi.org/10.1016/j.jsv.2006.10.011.
2. **Carrella, A.; Brennan, M. J.; Kovacic, I.;** et al. 2009. On the force transmissibility of a vibration isolator with quasi-zero-stiffness, Journal of Sound and Vibration 322: 707-717.
   https://doi.org/10.1016/j.jsv.2008.11.034.
3. **Ivana, K.; Michael, J. B.; Timothy, P W.** 2008, A study of a nonlinear vibration isolator with a quasi-zero stiffness characteristic, Journal of Sound and Vibration 315:700-711.
   https://doi.org/10.1016/j.jsv.2007.12.019.
4. **Liu, X.; Huang, X.; Hua, H.** 2013. On the characteristics of a quasi-zero stiffness isolator using Euler buckled beam as negative stiffness corrector, Journal of Sound and Vibration 322: 3359-3376.
   https://doi.org/10.1016/j.jsv.2012.10.037.
5. **Zhou, J.; Wang, X.; Xu, D.;** et al. 2015. Nonlinear dynamic characteristics of a quasi-zero stiffness vibration isolator with cam–roller–spring mechanisms, Journal of Sound and Vibration 346: 53-69.
   https://doi.org/10.1016/j.jsv.2015.02.005.
6. **Kovacic, I.; Brennan, M. J.; Lineton, B.** 2009. Effect of a static force on the dynamic behavior of a harmonically excited quasi-zero stiffness system, Journal of Sound and Vibration 325: 870-883.
   https://doi.org/10.1016/j.jsv.2009.03.036.
7. **Lan, C. C.; Yang, S. A.; Wu, Y. S.** 2014. Design and experiment of a compact quasi-zero-stiffness isolator capable of a wide range of loads, Journal of Sound and Vibration 333: 4843-4858.
   https://doi.org/10.1016/j.jsv.2014.05.009.
8. **Sun, X.; Xu, J.; Jing, X.;** et al. 2014. Beneficial performance of a quasi-zero-stiffness vibration isolator with time-delayed active control, International Journal of Mechanical Sciences (82): 32-40.
   https://doi.org/10.1016/j.ijmecsci.2014.03.002.
9. **Li, Y.; Xu, D.** 2017. Vibration attenuation of high dimensional quasi-zero stiffness floating raft system, International Journal of Mechanical Sciences (126): 186-195.
   https://doi.org/10.1016/j.ijmecsci.2017.03.029.
10. **Robertson, W. S.; Kidner, M. R. F.; Cazzolato, B. S.;** et al. 2009. Theoretical design parameters for a quasi-zero stiffness magnetic spring for vibration isolation, Journal of Sound and Vibration (326): 88-103.
    https://doi.org/10.1016/j.jsv.2009.04.015.
11. **Xu, D.; Yu, Q.; Zhou, J.;** et al. 2013. Theoretical and experimental analyses of a nonlinear magnetic vibration isolator with quasi-zero-stiffness characteristic, Journal of Sound and Vibration (332): 3377-3389.
    https://doi.org/10.1016/j.jsv.2013.01.034.
12. **Hao, Z.; Cao, Q.** 2015. The isolation characteristics of an archetypal dynamical model with stable-quasi-zero-stiffness, Journal of Sound and Vibration (340): 61-79.
    https://doi.org/10.1016/j.jsv.2014.11.038.
13. **Zhou, J.; Xiao, Q.; Xu, D.;** et al. 2017. A novel quasi-zero-stiffness strut and its applications in six-degree-of-freedom vibration isolation platform, Journal of Sound and Vibration (394): 59-74.
    https://doi.org/10.1016/j.jsv.2017.01.021.
14. **Zhu, T.; Cazzolato, B.; Robertson, W. S. P.;** et al. 2015. Vibration isolation using six degree-of-freedom quasi-zero stiffness magnetic levitation, Journal of Sound and Vibration (358): 48-73.
    https://doi.org/10.1016/j.jsv.2015.07.013.
15. **Xu, D.; Cheng, C.; Zhou, J.** 2014. Design and Characteristic Analysis of a Buckling Plate Vibration Isolator with Quasi zero-stiffness, Journal of Hunan University (Natural Sciences) 41(8): 17-22.
16. **Xu, D.; Zhao, Z.; Zhou, J.** 2013. Design and Characteristic Analysis of a Buckling Plate Vibration Isolator with Quasi zero-stiffness, Journal of Hunan University (Natural Sciences) 40(6): 47-52.
    https://doi.org/10.3969/j.issn.1674-2974.2013.06.008.
17. **Lim, C. W.; Wu, B. S.** 2003. A new analytical approach to the Duffing-harmonic oscillator, Physics Letters A (311): 365-373.
    https://doi.org/10.1016/S0375-9601(03)00513-9.

B. Kang, H. Li, Z. Zhang, H. Zhou

A STUDY OF A RUZICKA VIBRATION ISOLATOR MODEL WITH HIGH-STATIC-LOW-DYNAMIC CHARACTERISTIC

S u m m a r y

This paper studies a Ruzicka vibration isolator model with high-static-low-dynamic characteristic. Firstly, we analyze mechanical property of the quasi-zero stiffness spring which is composed of a cylinder and get an approximate expression of the spring's static force. This kind of spring is the main part of a high-static-low-dynamic vibra-

tion isolator. Secondly, a Ruzicka high-static-low-dynamic vibration isolator with Duffing equation is put forward, which is a combination of a Ruzicka vibration isolator and a high-static-low-dynamic vibration isolator. In the calculation process of solving its amplitude-frequency characteristic, a new method — Harmonic Equivalent Linearization Method — is used, in which the equivalent linearization algorithm is introduced into Harmonic Balance Method. This method could greatly simplify the calculation process and gives the same result as Harmonic Balance Method. Finally, the effects of additional stiffness, damping and excitation amplitude on nonlinear amplitude-frequency characteristic are investigated numerically, and also verified that the stable solutions of simulation and equation are similar. The results show that the Ruzicka high-static-low-dynamic vibration isolator is suitable for small amplitude vibration. The appropriate additional stiffness and damping ratio can change the resonance band of the amplitude-frequency characteristic curve. Therefore, the resonance can be suppressed by controlling the initial state of vibration.